Photochemical & Photobiological Sciences

RSC Publishing

PAPER

View Article Online
View Journal | View Issue

Photoinduced processes in a dyad made of a linear and an angular perylene bisimide

Cite this: *Photochem. Photobiol. Sci.*, 2013, **12**, 2137

Lucia Flamigni,*[a] Alberto Zanelli,[a] Heinz Langhals*[b] and Bernd Böck[b]

Received 3rd July 2013,
Accepted 14th September 2013

DOI: 10.1039/c3pp50211b

www.rsc.org/pps

A dyad (**PI0–PIa**) made of a linear (**PI0**) and an angular (**PIa**) perylene biscarboximide is synthesized and its spectroscopic, electrochemical and photophysical properties investigated in solvents of various polarity. **PIa** is characterized by a high intersystem crossing. The spectroscopy and electrochemistry data point to a modest electronic coupling. LUMO–LUMO electron transfer from the singlet excited state **PI0–^{1}PIa** is thermodynamically feasible in polar solvents but its occurrence is precluded by a very fast energy transfer to yield **^{1}PI0–PIa**, $k_{en} \geq 10^{11}$ s^{-1}. A HOMO–HOMO electron transfer in the latter state in polar solvents is precluded by the poor driving force, the reaction being unable to compete with the radiative deactivation of the excited state. The efficient energy transfer process is quantitatively examined in the frame of current theories and ascribed to a dipole–dipole (Förster) mechanism.

Published on 07 October 2013.

Introduction

Exploitation of solar energy is not only a hot research topic but is becoming an obligation in order to preserve our planet intact. Artificial photosynthesis, a field aiming at converting light energy into chemical (electrochemical) potential by mimicking the basic aspects of natural photosynthesis, is one of the subjects which might provide answers to this problem.[1] Fundamental aspects on the processes involved, photoinduced energy and electron transfer, have been extensively explored in multi-partite molecular structures mostly mimicking the naturally occurring pigments, tetrapyrroles.[2] However, the interest for alternative chromophores which might lead to even more satisfactory results is very active.[3] Among the new potentially successful dyes, aromatic carboxylic bisimides have an important position and their use in assemblies for the collection and conversion of light energy has become widespread.[4,5] Among those, perylene-3,4:9,10-tetracarboxylic bisimides, perylene dyes such as **PI0** (Fig. 1) have become of great interest for their high quantum yield of fluorescence (a precious tool in mechanistic studies), their extraordinarily high photostability, their electron conducting properties and their rich phenomenology upon aggregation.[6]

Very recently we have reported on the angular bisimide **PIa**.[7–9] This new perylene bisimide derivative is more electron rich than **PI0**, in addition to a still high fluorescence quantum yield (ϕ_{fl} = 0.37 ± 0.03) **PIa** is able to undergo efficient intersystem crossing. Therefore, at variance with most perylene bisimides, it displays typical triplet state photoreactivity as singlet oxygen photosensitization[8] with ϕ_{Δ} = 0.68 ± 0.02, and low temperature phosphorescence at 692 nm.[9] **PIa** has also

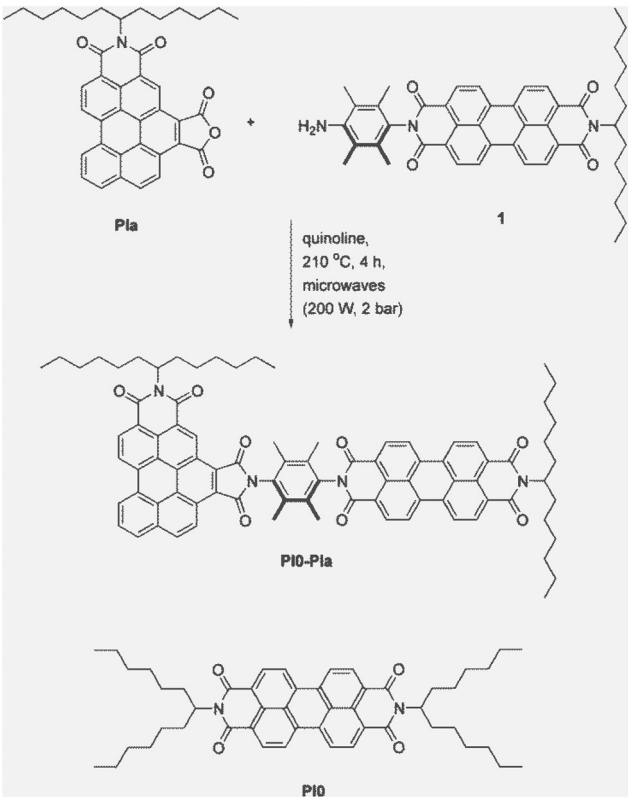

Fig. 1 Synthesis of the dyad **PI0–PIa** and component units **PIa** and **PI0**.

[a]*Istituto per la Sintesi Organica e Fotoreattivita' (ISOF), CNR, Via P. Gobetti 101, 40129 Bologna, Italy. E-mail: lucia.flamigni@isof.cnr.it*
[b]*Department of Chemistry, LMU University of Munich, Butenandtstr. 13, D-81377 Munich, Germany. E-mail: Langhals@lrz.uni-muenchen.de*

Published on 07 October 2013.

been used as an electron donor in a dyad comprising corrole and has provided a charge separated state lifetime of several microseconds, an impressive result if one considers the simple structure of the array and the close proximity of the reactants.[10] The reason for such behaviour has to be ascribed to a quite high driving force, of the order of 2 eV, together with a very small rearrangement of the molecular structure from the charge separated state to the ground state. This results in a reaction with the ΔG^0 largely exceeding the reorganizational energy and as such falling in the "inverted" region and, according to Marcus theory, in a slow recombination reaction.[11]

Here we report on the synthesis, electrochemical and photophysical characterization of a new dyad (**PI0–PIa**) (Fig. 1) derived from two different perylene bisimides, the most classical **PI0** which has been extensively studied in many laboratories, including ours,[6,12] and the angular bisimide **PIa**, discussed above. **PI0** is a well-known electron acceptor and in addition to the impressive fluorescence has, among others, the advantage that the related anion radical provides remarkably strong spectra with fingerprints in the Vis and NIR spectral regions.[12] The new perylene bisimide derivative **PIa**, as described above has complementary characteristics to those of **PI0**, and can act as an energy donor or an electron donor in a perpendicular dyad with **PI0**. This system is closely related to a recently reported perpendicular dyad where a benzoperylene tris-carboximide is linked to **PI0** and exhibits FRET in spite of orthogonal transition dipole moments.[13,14] We intend to ascertain whether electron transfer can play any role in the dynamics of the excited state of the dyad and, in order to take advantage of the important effect of solvent polarity on electron transfer reactions, we studied the photoreactivity of the dyad in a series of solvents of increasing polarity, from apolar toluene to moderately polar dichloromethane to polar benzonitrile.

Results and discussion

Synthesis

PIa[7] was condensed in quinoline with perylene amine **1**.[14] The application of micro waves gave appreciably better yields (50%) than a simple thermal condensation.

Spectroscopy and photophysics

The systems examined are **PI0–PIa** and the component models **PIa** and **PI0**. When we refer to the component units in the dyad **PI0–PIa**, a non-bold notation PIa and PI0, will be used. The absorption spectra of the dyad and of the component units are reported for toluene (TL) solutions in Fig. 2. The absorption spectra in the other solvents used, dichloromethane (DCM) and benzonitrile (BN) are almost identical to that in TL, with the sample spectra in BN displaying a very modest bathochromic shift of *ca.* 2 nm (data not shown). **PI0–PIa** has spectroscopic absorption features which are an almost perfect superposition to those of the components if one makes

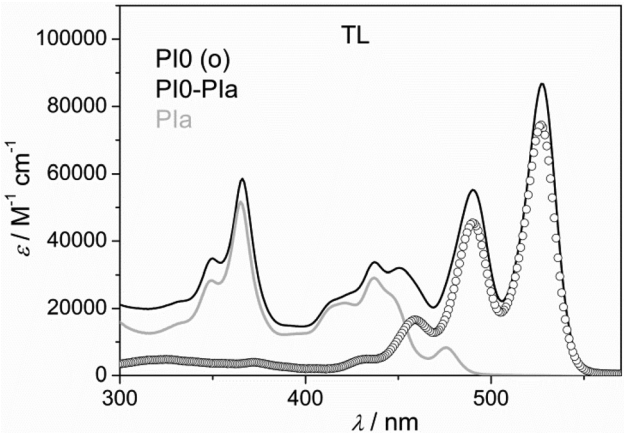

Fig. 2 Absorption spectra in molar absorption coefficient unit of the dyad and of the components.

allowance for errors in the molar absorption coefficients and for less than 2 nm hypsochromic shift in the dyad peaks. This is a clear indication of the absence of sizeable electronic interactions between the units in the ground state.

The fluorescence spectrum of the dyad, irrespective of the excitation wavelength is coincident with the spectrum of **PI0**, the component at lower energy, whereas the luminescence of PIa component is totally quenched. This is quite expected if an efficient process of energy transfer from the higher energy **PIa** to the lower energy **PI0** is operative, but a similar outcome would be obtained also if the two parallel processes, energy and electron transfer would occur. Obviously, in the first case a luminescence yield accounting for all the photons absorbed by the dyad (also by the PIa component) would be expected, whereas in the second a lower emission quantum yield, not fully accounting for the photons absorbed by the dyad would be found. It is therefore important to examine the data from a quantitative point of view in order to have an indication on the two possible mechanisms. Whereas it is possible to selectively excite the PI0 component at wavelength above 490 nm, excitation of PIa unit can be only predominant at 365 nm. The results of excitation at these two different wavelengths of the dyad **PI0–PIa** in TL solution and of the component models are reported in Fig. 3A and B respectively.

The absorbance of the model components **PI0** and **PIa** is adjusted to absorb the same number of photons as in the array, see inset in Fig. 3A. Upon excitation at 366 nm, Fig. 3A, the luminescence of the dyad is enhanced by a factor of 10 compared to the model **PI0**. This corresponds to the ratio between the absorbance of **PI0** and the absorbance of the dyad, indicating that all photons absorbed by PIa unit in **PI0–PIa** are conveyed to PI0. From this, an almost 100% efficiency in sensitization by PIa to PI0 can be calculated. Upon selective excitation of PI0 unit in **PI0–PIa** at 490 nm in TL, Fig. 3B, the luminescence yield is the same as that of the model, within experimental error. This testifies that in TL solutions upon excitation of the PIa unit there is a quantitative energy transfer to the PI0 acceptor unit and upon excitation of the PI0 moiety

 This journal is © The Royal Society of Chemistry and Owner Societies 2013

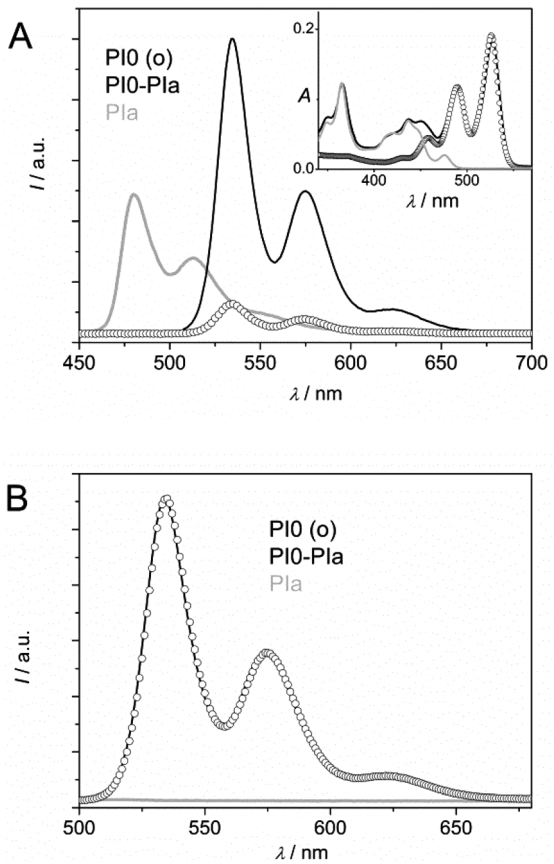

Fig. 3 Uncorrected luminescence spectra in TL of **PI0–PIa** and models upon excitation at 366 nm (A) and 490 nm (B). The absorption spectra of the examined solutions are reported as an inset in panel A.

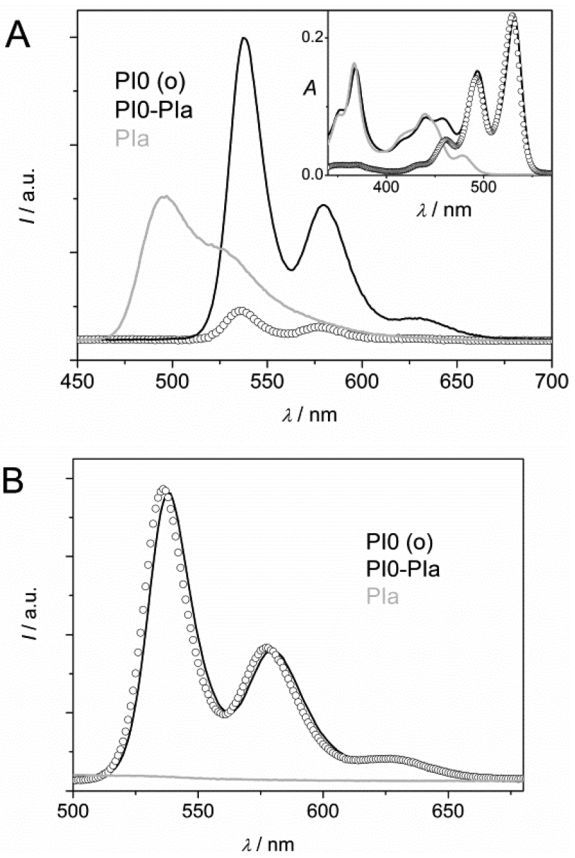

Fig. 4 Uncorrected luminescence spectra in BN of **PI0–PIa** and models upon excitation at 367 nm (A) and 493 nm (B). The absorption spectra of the examined solutions are reported as an inset in panel A.

Published on 07 October 2013.

there is no further reactivity but a deactivation of this unit as in the model.

It is well known that polarity of the solvent can greatly enhance electron transfer, whereas it is, in general, much less effective on energy transfer rates.[11,15,16] The reason is that the charge separated state formed by the transfer of an electron from the more electropositive to the more electronegative component can be stabilized more in polar solvents, resulting in a net increase of driving force for electron transfer. Therefore, the same experiment was repeated in DCM and BN solutions, where the driving force for charge separation is expected to increase and hence favor electron transfer. The results are rather similar to that of TL solutions, and as an example the data of an experiment in the most polar BN solutions are shown in Fig. 4.

The results of excitation in the dyad on the maximum of the UV band of PIa at 367 nm, Fig. 4A, indicate that the intensity of the PI0 component emission is also enhanced by 10.8 times compared to a model absorbing approximately 11% of the photons of the dyad. This is indicative, within experimental uncertainty, of the fact that all photons absorbed by the PIa unit are conveyed into the PI0 component. Excitation at 493 at the PI0 unit maximum (Fig. 4B) produces the same fluorescence as an isoabsorbing solution of the model **PI0**. So even in polar BN, where electron transfer should be favored, energy transfer is found to be quantitative.

This is confirmed by the excitation spectra recorded on the emission band of PI0 at 565 nm in different solvents, which are an almost perfect superposition of the absorption spectra of the dyad, Fig. 5. It seems that, in spite of the more electron rich nature of the component PIa, the energy stored in the excited state (*ca.* 2.56 eV) is not sufficient to promote electron transfer even in the most polar solvents.

In order to confirm this, we performed a series of time resolved luminescence and absorption experiments. A picosecond time resolved luminescence study indicates that the luminescence of the donor PIa is quenched in the dyad in all solvents to a lifetime $\leq$10 ps, the resolution of the apparatus, against a natural lifetime of **PIa** of 7–8 ns, Table 1. On the other hand, the rise of the luminescence localized on the energy acceptor PI0, is within the pulse duration. This allowed us to derive a value for a lower limit for the rate of energy transfer: $k_{en} \geq 10^{11}$ s^{-1}. The luminescence data for the dyad and the components at room temperature for the various solvents and at 77 K for TL, are collected in Table 1.

Pump and probe spectroscopy experiments with picosecond resolution were also performed in order to detect absorbing species, *e.g.* radicals. Transient absorption detected in the

model components and in the dyad is reported in Fig. 6 for the various solvents. **PI0** solutions display a spectrum ascribable to the excited singlet state, ^{1}**PI0**. This has well characterized features, quite different in the various solvents, as already described in former reports.[12f,h] Maxima at 690 and 850 nm in TL, a single sharp maximum at 710 nm in DCM and a single broad maximum at 725 nm in BN are seen, (Fig. 6B). **PIa** has a very weak band with a broad maximum around 570 nm in all solvents. The spectrum registered in the dyad after a 35 ps pulse, continuous line in Fig. 6, is exactly superimposing the spectrum detected in isoabsorbing solutions of **PI0** in the same solvent. Furthermore, the time evolution of the signal is similar for the dyad and the model: the time window accessible in the pump and probe experiment is only 3.3 ns and therefore unsuitable to determine lifetime of the order of several nanoseconds, as the present ones, however, the lifetime measured in **PI0** and **PI0–PIa** are totally consistent with the values of 4 and 3.7 ± 0.1 measured by luminescence techniques (Table 1). This clearly confirms that the only species present in the dyad solution is the excited singlet state localized on PI0, formed as a result of energy transfer from the PIa moiety in the dyad. No trace of the radical anion **PI0**$^-$, which has a well characterized absorption spectrum with strong bands at 710, 800 and 960 nm is present.[12c–g] Therefore, we can state with confidence that the only process occurring is energy transfer.

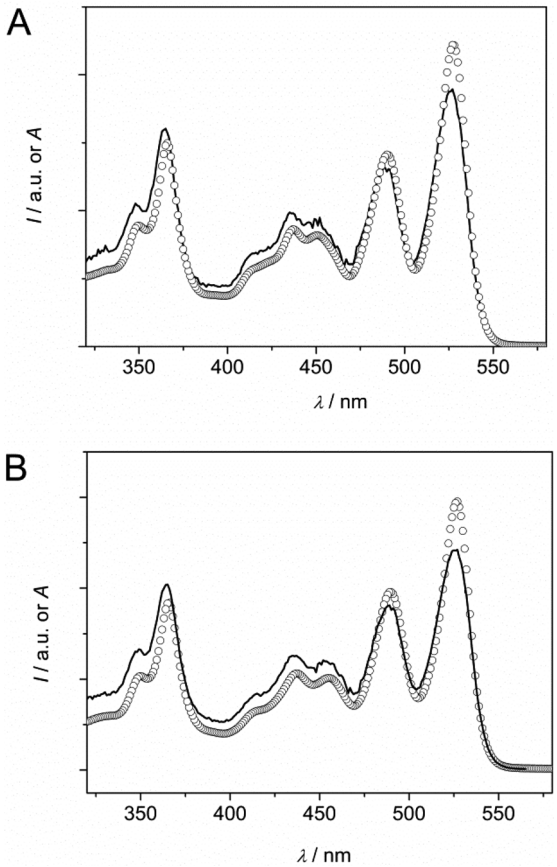

Fig. 5 Excitation spectra registered at λ_{em} = 565 nm of dyad **PI0–PIa** compared to normalized absorption spectra in TL (A) and DCM (B).

Electrochemistry

In order to have further information on the dynamics of the processes we performed electrochemical investigations by cyclic voltammetry. Fig. 7 shows the voltammograms of the model perylene carboximides and their dyad. Both **PI0**[12f] and **PIa**[8] show two quasi-reversible reduction waves. Those of **PIa** are shifted more than 300 mV toward more negative potentials with respect to those of **PI0** indicating that the angular geometry of the carboximides breaks the conjugation of the LUMO.

Published on 07 October 2013.

Table 1 Luminescence data for the examined compounds in dichloromethane, toluene and benzonitrile

	295 K				77 K		
	λ_{max} [a]/nm	Φ_{fl} [b]	Φ_{fl} [c]	τ [d]/ns	λ_{max} [a]/nm	τ [d]/ns	E/eV [e]
TL (ε = 2.4)							
PI0 [f]	534, 574, 622		0.92	4.0	543, 587, 638	4.0	2.28
PIa [f]	481, 512	0.37		8.4	483, 516, 555 (sh)	10.0	2.56
					686, 764, 862		1.79 [i]
PI0–PIa	532, 572, 622	0.90	0.95	≤0.01 [g]; 3.8 [h]	545, 558, 639	3.7	2.27
DCM (ε = 8.9)							
PI0 [f]	529, 571, 629		0.99	4.0			
PIa [f]	489, 520 (sh)	0.38 [b]		6.7			
PI0–PIa	532, 574, 625	0.97	0.99	≤0.01 [g]; 3.7 [h]			
BN (ε = 25.9)							
PI0 [f]	536, 578, 627		0.98	4.0			
PIa [f]	496, 522 (sh)	0.40 [b]		8.4			
PI0–PIa	538, 579, 628	1.0	0.95	≤0.01 [g]; 3.6 [h]			

[a] Data from uncorrected spectra. [b] Excitation on the UV band of PIa at 366 nm in TL and DCM and 367 nm in BN. [c] Excitation on the band of PI0 at 490 in TL and DCM and 493 in BN. [d] Excitation at 465 nm for nanosecond and at 355 nm for picosecond determinations. [e] From spectra recorded at 77 K. [f] From ref. 8. [g] Lifetime measured on the PIa band at *ca.* 480 nm. [h] Lifetime measured on the PI0 band at 570 nm. [i] Derived from phosphorescence bands, from ref. 9.

 This journal is © The Royal Society of Chemistry and Owner Societies 2013

Published on 07 October 2013.

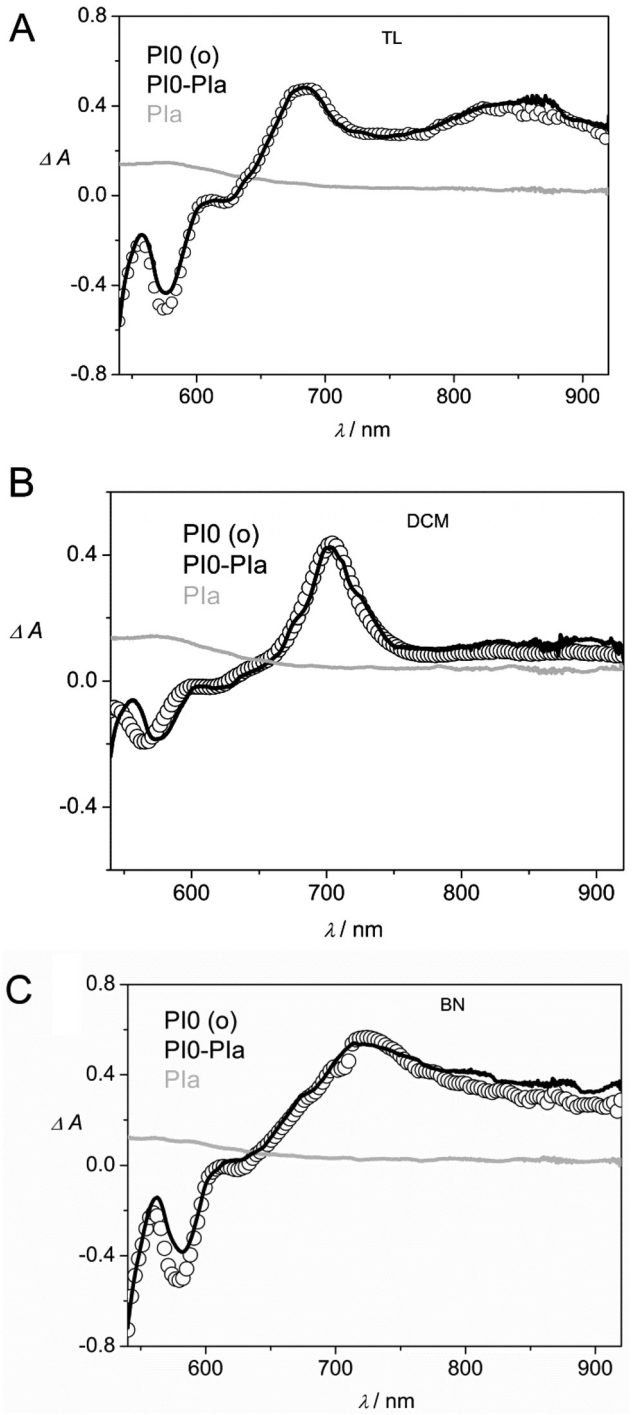

Fig. 6 Spectra detected at the end of the 35 ps laser pulse for the models and dyad **PI0–PIa** in various solvents after excitation at 355 nm.

The dyad shows four reduction waves 90–40 mV less negative than that of its components, indicating a poor conjugation between the two parts of the dyad. On the other hand, the oxidation potential of **PI0**, **PIa** and their dyad appears the same, even if this determination is affected by the uncertainty due to the overlapping to the breakdown current of the electrolyte. Table 2 reports the redox potential distribution of the models and dyad.

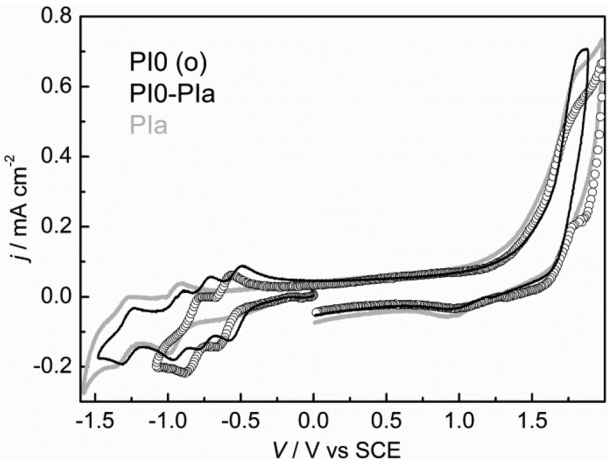

Fig. 7 Cyclic voltammetries of **PI0** (2.2×10^{-4} M), **PIa** (1.3×10^{-4} M) and **PI0–PIa** (1.7×10^{-4} M) at 0.1 V s^{-1} in DCM 0.1 M TBAP.

Table 2 Redox potentials (V *vs.* SCE) in DCM 0.1 M TBAP

	E°_{red1}	E°_{red2}	E°_{red3}	E°_{red4}	E°_{ox1}
PI0	−0.62	−0.83			1.77
PIa			−0.96	−1.30	1.75
PI0–PIa	−0.53	−0.74	−0.89	−1.26	1.75

Photoinduced processes

An approximate energy level diagram for dyad **PI0–PIa** is shown in Fig. 8. The data of Table 1 and those from electrochemistry, Table 2, are used to determine the energy levels of excited states and charge separated states (CS), respectively.

The CS at lower energy is the one with reduced PI0 and oxidized PIa moieties (**PI0**$^{-}$**–PIa**$^{+}$), see the Electrochemistry section. In order to determine the energy level of CS, the electrochemical potentials need to be corrected by taking into account the Coulombic interaction term and the ion solvation energy based on the Born dielectric continuum model, when the solvent is different from the one used in the electrochemical determinations. The correction of the electrochemical potential can be done according to the simplified following equation which provides the energy for charge separation reaction (relative to the neutral ground state):[15]

$$\Delta G^{0} = E_{ox} - E_{red} - (14.32/R_{DA}\varepsilon_{S}) + 14.32\ (1/2r_{D} + 1/2r_{A})\ (1/\varepsilon_{S} - 1/\varepsilon_{P}) \quad (1)$$

In the present case, ε_S = 2.4, ε_S = ε_P = 8.9 and ε_S = 25.9 are the dielectric constants of TL, DCM and BN, respectively. The center to center donor–acceptor distance calculated after energy minimization is 17 Å, whereas the radii are taken as r_A = 6 Å (**PI0**) and r_D = 5 Å (**PIa**).

The results of the calculation indicate for **PI0**$^{-}$**–PIa**$^{+}$ a value of *ca.* 2.7 eV in TL, 2.2 eV in DCM and 2.1 eV in BN. Therefore, see Fig. 8, the CS states in polar solvents are well below the energy level of the excited state of **PI0–PIa** localized on PIa

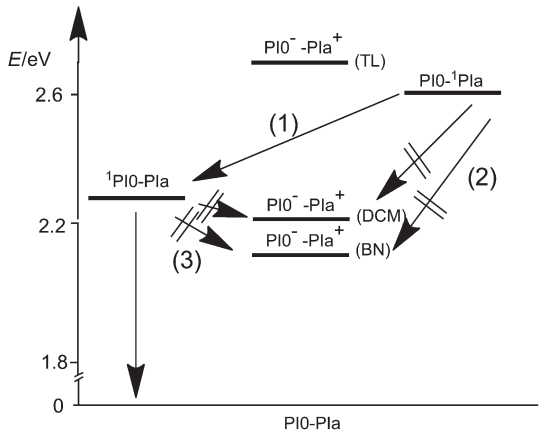

Fig. 8 Schematic energy level diagram of dyad **PI0–PIa**.

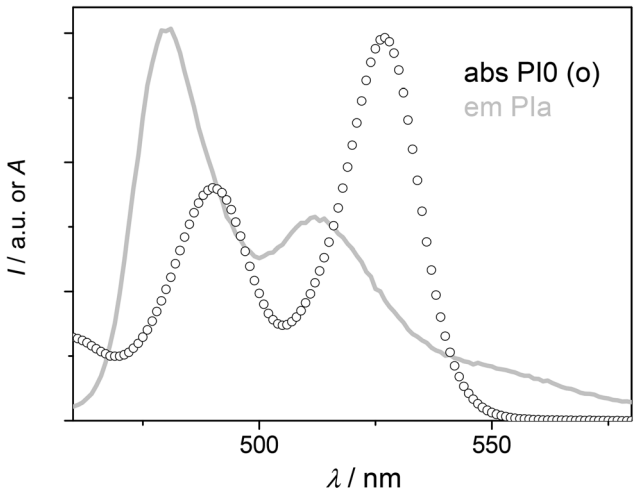

Fig. 9 Normalized spectra of **PIa** donor emission and of **PI0** acceptor absorption.

(**PI0–^{1}PIa**) and similar to or slightly lower than the energy level of the lowest singlet excited state of **PI0–PIa**, localized on PI0 (**^{1}PI0–PIa**). A HOMO–HOMO electron transfer (process **3**) in the latter excited state is not expected during the short lifetime of the state (3.7 ± 0.1 ns) on the basis of the very low driving force for the charge separation reaction, *ca.* 0.1–0.2 eV. In contrast, a LUMO–LUMO electron transfer (process **2**) could take place from the **PI0–^{1}PIa** excited state in the two more polar solvents. These reactions in fact display a driving force of the order of 0.36 for DCM and 0.46 for BN, sufficient to grant a fast rate. However, from the presented data we can positively state that electron transfer is prevented by a very fast competing energy transfer (process **1**) occurring from the excited state localized on PIa, **PI0–^{1}PIa**, to that localized on PI0, **^{1}PI0–PIa**. Once the latter excited state is formed, its reactivity is essentially identical to that of the model **PI0**, except for a small decrease in lifetime, Table 1. This modest reduction in lifetime, of the order or lower than 10%, can be ascribed to a slight change of radiative rate constant in the dyad, as the constancy of emission quantum yield testifies, rather than to an intra-molecular reaction of **^{1}PI0–PIa** as would be process **3**.

We intend to explore the nature of the energy transfer process **1** from **PI0–^{1}PIa** to **^{1}PI0–PIa**, for which a rate $\geq 10^{11}$ s^{-1} was determined. Singlet–singlet energy transfer can take place based on: (i) a dipole–dipole interaction between the energy donor and the energy acceptor (Förster mechanism);[17] (ii) a double electron exchange involving the transfer of the electron from the LUMO of the excited donor to the empty LUMO of the acceptor with a concomitant transfer of an electron from the HOMO of the acceptor to the HOMO of the donor (Dexter mechanism).[18] When an extended overlap between the emission of a strongly luminescent donor and the absorption of a strongly absorbing acceptor exists, see Fig. 9, an ultrafast energy transfer occurring *via* a Förster mechanism is generally favored. The rate of a Förster process (in s^{-1}) can be calculated from the following equation:[17]

$$k_{en}^{F} = \frac{8.8 \times 10^{23} \kappa^2 \phi}{n^4 \tau d_{DA}^6} J^F \qquad (2)$$

where ϕ and τ are the emission quantum yield and lifetime in nanoseconds of **PIa** listed in Table 1, d_{DA} is the donor–acceptor center-to-center distance, 17 Å, n is the refractive index of the solvent and κ^2 is a geometrical factor. J^F is the Förster overlap integral which can be calculated from the emission spectrum of the donor **PIa** and the absorption spectrum of the acceptor **PI0** according to eqn (3).

$$J^F = \frac{\int F(\bar{\nu})\varepsilon(\bar{\nu})/\bar{\nu}^4 \mathrm{d}\bar{\nu}}{\int F(\bar{\nu})\mathrm{d}\bar{\nu}} \qquad (3)$$

A J^F of 1.9×10^{-13} cm^3 M^{-1} is calculated in TL which, by substituting values in eqn (2) leads to $k_{en}^F = (6.1 \times 10^{10}\ \mathrm{s}^{-1})\ \kappa^2$. Now, assuming that the transition dipole orientation in PIa is of *ca.* 45° with respect to the line connecting the centers of the donor and of the acceptor in the dyad, a κ^2 value of 2 can be derived.[19,20] This κ^2 value allows to calculate the rate of energy transfer $k_{en}^F = 1.2 \times 10^{11}$ s^{-1} which is in agreement with the experimental value of $k_{en} \geq 10^{11}$ s^{-1}.

On the other hand, by assuming the energy transfer occurring by an electron exchange mechanism (Dexter), the following equations can be used to estimate H, the intercomponent electronic interaction, from the observed rate constant:[18]

$$k_{en}^D = \frac{4\pi^2 H^2}{h} J^D \qquad (4)$$

$$J^D = \frac{\int F(\bar{\nu})\varepsilon(\bar{\nu})\mathrm{d}\bar{\nu}}{\int F(\bar{\nu})\mathrm{d}\bar{\nu} \int \varepsilon(\bar{\nu})\mathrm{d}\bar{\nu}} \qquad (5)$$

J^D, the Dexter integral overlap, can be evaluated from the absorption spectrum of the complexed acceptor and from the luminescence spectrum of the donors normalized for the absorption of the acceptor. The calculated value of J^D is 2.58×10^{-4} cm and by introducing this value in eqn (4), an intercomponent electronic interaction $H \geq 18$ cm^{-1} is derived. The order of magnitude of such coupling is sizeable, higher than expected for weakly interacting components such as the present one. This result further supports the interpretation of

Published on 07 October 2013.

This journal is © The Royal Society of Chemistry and Owner Societies 2013

an energy transfer mechanism occurring by a dipole–dipole interaction.

Conclusion

We have examined a new dyad containing a linear perylene biscarboximide and an angular benzoperylene biscarboximide. The latter component has a higher spectroscopic energy of the emitting excited singlet, is more electron rich than the linear one and displays efficient triplet reactivity. The photoinduced process is characterized by an efficient Förster energy transfer ($k_{en} \geq 10^{11}$ s^{-1}) from the excited state localized on the angular perylene derivative, **PI0–^{1}PIa** to the one localized on the linear one, **^{1}PI0–PIa**. Inter system crossing with the formation of triplet states is important for angular benzoperylene biscarboximides but in the present case efficient energy transfer prevents the occurrence of this process. Electron transfer leading to the charge separated state (CS) **PI0$^-$–PIa$^+$**, thermodynamically feasible in polar solvents, cannot compete with the fast energy transfer. It is clearly shown that the dynamics of excited states in this dyad is ruled by energy transfer processes. Light energy accumulation in the low-energy component and re-emission, occurring by an almost unity quantum yield is of interest for the construction of more complex, highly efficient antennas for light-harvesting.

Experimental

N^2-(1-Hexylheptyl)-*N*^{1}-[*N*-(1-hexylheptyl)-*N*′-(2,3,5,6-tetramethylphenyl-4-yl)perylene-3,4,9,10-bis(dicarboximide)]benzo[*ghi*]-perylene-3,4,6,7-bis(dicarboximide) (**PI0–PIa**): *N*-(1-hexylheptyl)-benzo[*ghi*]perylene-3,4,6,7-tetracarboxylic-3,4-dicarboximide-6,7-anhydride (**PIa**, 55.4 mg, 92.7 μmol) and *N*-(1-hexylheptyl)-*N*′-(4-amino-2,3,5,6-tetramethylphenyl)perylene-3,4,9,10-bis-(dicarboximide) (**1**, 100 mg, 139 μmol) were dissolved in quinoline (3.00 mL), heated in a microwave apparatus (210 °C, 200 W, 2.0 bar) for 4 h, poured into 2 M aqueous HCl (250 mL) and extracted with chloroform until a colourless organic phase. The combined chloroform phases were extracted with 2 M aqueous HCl (3 × 150 mL) and the latter extracted with chloroform. The combined organic phases were dried with magnesium sulphate and evaporated *in vacuo*. The residue was purified by column separation (silica gel 63–200 μm, $CHCl_3$–EtOH 50 : 1, intensely reddish-orange fluorescent fraction after a yellow, weakly fluorescent forerun and a second column separation with $CHCl_3$–EtOH 100 : 1), dissolved in minimal amount of chloroform and precipitated with methanol. Yield 64.0 mg (53%) red powder, m.p. 317–321 °C. R_f (silica gel, $CHCl_3$–EtOH 50 : 1): 0.18. IR (ATR): $\tilde{\nu}$ = 3362.2 (w), 3074.2 (w), 2953.9 (s), 2921.7 (vs), 2852.6 (vs), 1714.9 (m), 1660.0 (m), 1632.2 (m), 1593.4 (m), 1461.0 (s), 1404.5 (m), 1377.2 (m), 1340.0 (m), 1260.6 (m), 1097.0 (m), 1023.5 (m), 967.5 (w), 808.6 (s), 767.3 (w), 746.7 (m), 721.7 (m), 696.2 (m), 658.4 cm^{-1} (w). ^{1}H NMR (600 MHz, $CDCl_3$): δ = 0.74–0.78 (m, 12H, CH_2CH_3), 1.11–1.24 (m, 32H, $CH_2CH_2CH_2CH_2CH_3$), 1.77–1.85 (m, 2H, $CHCH_2$), 1.86–1.94 (m, 2H, $CHCH_2$), 2.14 (s, 6H, CCH_3), 2.17–2.23 (m, 2H, $CHCH_2$), 2,26 (s, 6H, CCH_3), 2.28–2.37 (m, 2H, $CHCH_2$), 5.10–5.16 (m, 1H, NC*H*), 5.23–5.31 (m, 1H, NC*H*), 8.21 (t, ^3J = 7.7 Hz, 1H, H_{arom}), 8.40–8.44 (m, 2H, H_{arom}), 8.62–8.68 (m, 5H, H_{arom}), 8.74–8.78 (m, 2H, H_{arom}), 8.96–9.05 (m, 2H, H_{arom}), 9.16 (d, ^3J = 7.7 Hz, 1H, H_{arom}), 9.17 (d, ^3J = 8.6 Hz, 1H, H_{arom}), 9.41 (d, ^3J = 8.9 Hz, 1H, H_{arom}), 10.43 ppm (br. d, ^3J = 20.4 Hz, 1H, CC*H*CO). ^{13}C NMR (150 MHz, $CDCl_3$): δ = 14.0, 15.4, 15.9, 22.6, 22.7, 26.9, 27.0, 29.2, 29.3, 29.5, 31.7, 31.8, 31.9, 32.4, 54.8, 55.0, 122.1, 122.9, 123.2, 123.3, 123.4, 123.7, 124.0, 124.9, 125.3, 126.5, 126.8, 127.1, 127.2, 128.5, 128.8, 129.6, 130.1, 130.2, 130.5, 132.0, 132.1, 132.3, 132.4, 132.8, 134.3, 134.4, 134.8, 135.3, 162.8, 168.2 ppm. UV/Vis ($CHCl_3$): λ_{max} (E_{rel}) = 261.6 (0.75), 350.4 (0.38), 366.4 (0.59), 438.8 (0.37), 456.0 (0.37), 491.0 (0.66), 527.8 (1.00). Fluorescence ($CHCl_3$): λ_{max} (I_{rel}) = 535.9 (1.00), 578.7 (0.51), 628.7 (0.11). MS (FAB$^+$): *m*/*z* (%) = 1300 (3) $[M + H]^+$, 1299 (1) $[M]^+$, 1298 (1) $[M - H]^+$, 1118 (2) $[M + H - C_{13}H_{26}]^+$, 1117 (1) $[M - C_{13}H_{26}]^+$, 1116 (0.5) $[M - H - C_{13}H_{26}]^+$, 936 (1) $[M + H - 2C_{13}H_{26}]^+$, 935 (1) $[M - 2C_{13}H_{26}]^+$, 934 (0.6) $[M - H - 2C_{13}H_{26}]^+$, 664 (2), 545 (2), 465 (27), 198 (100), 69 (66), 55 (93). HMRS (EI): calcd $C_{86}H_{83}N_4O_8$ $[M + H]^+$: 1299.6211, Gef. 1299.6190, Δ = 0.0021. $C_{86}H_{82}N_4O_8$ (1299.6): calcd C 79.48, H 6.36, N 4.31; found C 78.50, H 6.34, N: 4.14.

Electrochemistry

Cyclic voltammetries have been performed at room temperature, after Ar purging, using an AMEL 5000 electrochemical system in a homemade three compartment cell with semi-spherical Pt electrode (diameter 2 mm), Pt wire counter electrode and aqueous KCl Saturated Calomel Electrode (SCE = 0.47 V *vs.* ferrocene/ferricinium). The supporting electrolytes were DCM (C. Erba RPE, distilled over phosphoric anhydride and stored under Ar pressure) and 0.1 M tetrabutylammonium perchlorate (TBAP, Fluka, puriss. crystallized from methanol and vacuum dried). **PI0**,[21] **PIa** and **PI0–PIa** concentrations were ~1.5×10^{-4} M and the addition of a further ~50% was used to confirm the attribution of the oxidation wave to the samples.

Photophysics

The solvents used were spectroscopic grade toluene (C. Erba), spectroscopic grade dichloromethane (C. Erba), and HPLC grade benzonitrile (SIGMA-Aldrich). Absorption spectra were recorded using a Perkin-Elmer Lambda 9 spectrophotometer and the emission spectra, corrected for the wavelength sensitivity of the detection if not otherwise stated, were detected using a Spex Fluorolog II spectrofluorimeter equipped with a Hamamatsu R3896 photomultiplier. The luminescence quantum yields of the samples, ϕ_s, were evaluated against a standard with known emission quantum yield, ϕ_r, by comparing areas under the corrected luminescence spectra using the equation: $\phi_s/\phi_r = A_r n^2_s (\text{area})_s / A_s n^2_r (\text{area})_r$, where A is the absorbance, n is the refractive index of the solvent employed and s and r stand for sample and reference, respectively. The standard used was air-equilibrated quinine sulphate in 1 N

Published on 07 October 2013.

H_2SO_4 with an emission quantum yield ϕ_{fl} = 0.546 or **PI0** in DCM with ϕ_{fl} = 0.99. The absorbance of the solutions was <0.1 at the exciting wavelength.

Fluorescence lifetimes in the nanosecond region were detected using a Time Correlated Single Photon Counting apparatus (IBH) with excitation at 465 nm. A system based on a Streak Camera Hamamatsu C1587 equipped with M1952 and a Nd-YAG laser (Continuum PY62/10, 35 ps pulse, 1 mJ at 355 nm) was used for detecting luminescence with picosecond resolution.[22] Transient absorbance in the picosecond range made use of a pump and probe system based on a Nd-YAG laser (Continuum PY62/10, 35 ps pulse). The third harmonic (355 nm) with an energy of *ca.* 3 mJ per pulse was used to excite the samples whose absorbance at the excitation wavelength was *ca.* 0.5.[12d–g] Molecular dimensions and distances were estimated using Chem 3D Ultra 6.0 software after MM2 energy minimization. Computations of the integral overlap and of the rate for the energy-transfer processes according to the Förster mechanism were performed using Matlab 5.2.[23] Estimated errors are 10% on lifetimes, molar extinction coefficients and quantum yields. The working temperature, if not otherwise specified, is 295 ± 2 K.

Acknowledgements

We thank Italian CNR (MACOL, DP.04.010), the Eurocores project "Solarfueltandem" and PRIN 2010CX2TLM for financial support. We are grateful to Tommaso Fiorini (University of Bologna- Sede di Forli) for help with the use of Matlab 5.2.

Published on 07 October 2013.

References

1 (*a*) D. Gust, T. A. Moore and A. L. Moore, *Acc. Chem. Res.*, 2009, **42**, 1890–1898; (*b*) M. R. Wasielewski, *Acc. Chem. Res.*, 2009, **42**, 1910–1921; (*c*) J. J. Conception, R. L. House, J. M. Papanikolas and T. J. Meyer, *Proc. Natl. Acad. Sci. U. S. A.*, 2012, **109**, 15560–15564; (*d*) D. G. Nocera, *Acc. Chem. Res.*, 2012, **45**, 767–776.

2 (*a*) M. R. Wasielewski, *Chem. Rev.*, 1992, **92**, 435–461; (*b*) D. Gust, T. A. Moore and A. L. Moore, *Acc. Chem. Res.*, 2001, **34**, 40–48; (*c*) L. Flamigni, V. Heitz and J.-P. Sauvage, *Struct. Bonding*, 2006, **121**, 217–261; (*d*) A. Satake and Y. Kobuke, *Org. Biomol. Chem.*, 2007, **5**, 1679–1691; (*e*) *Multiporphyrin Arrays: Fundamental and applications*, ed. D. Kim, Pan Stanford Publishing Pte. Ltd, Singapore, 2012; (*f*) J. D. Megiatto, A. Antoniuk-Pablant, B. D. Sherman, G. Kodis, M. Gervaldo, T. A. Moore, A. L. Moore and D. Gust, *Proc. Natl. Acad. Sci. U. S. A.*, 2012, **109**, 15578–15583; (*g*) L. Flamigni, *J. Photochem. Photobiol., C*, 2007, **8**, 191–210; (*h*) L. Flamigni and D. T. Gryko, *Chem. Soc. Rev.*, 2009, **38**, 1635–1646.

3 (*a*) N. Martin, L. Sanchez, M. A. Herranz, B. Illescas and D. M. Guldi, *Acc. Chem. Res.*, 2007, **40**, 1015–1024; (*b*) L. Flamigni, J.-P. Collin and J.-P. Sauvage, *Acc. Chem. Res.*, 2008, **41**, 857–871; (*c*) A. Magnuson, M. Anderlund, O. Johansson, P. Lindblad, R. Lomoth, T. Polivka, S. Ott, K. Stensjö, S. Styring, V. Sundström and L. Hammarström, *Acc. Chem. Res.*, 2009, **42**, 1899–1909; (*d*) J. J. Concepcion, J. W. Jurss, M. K. Brennaman, P. G. Hoertz, A. O. T. Patrocinio, N. Y. M. Iha, J. L. Templeton and T. J. Meyer, *Acc. Chem. Res.*, 2009, **42**, 1954–1965; (*e*) H. Lemmetyinen, N. V. Tkachenko, A. Efimov and M. Niemi, *Phys. Chem. Chem. Phys.*, 2011, **13**, 397–412.

4 (*a*) M. P. O' Neil, M. P. Niemczyk, W. A. Svec, D. Gosztola, G. L. Gaines III and M. R. Wasielewski, *Science*, 1992, **257**, 63–65; (*b*) A. Osuka, S. Nakajima, K. Maruyama, N. Mataga, T. Asahi, I. Yamazaki, Y. Nishimura, T. Ohno and K. Nozaki, *J. Am. Chem. Soc.*, 1993, **115**, 4577–4589; (*c*) Q. Tan, D. Kuciauskas, S. Lin, S. Stone, A. More, T. A. More and D. Gust, *J. Phys. Chem. B*, 1997, **101**, 5214–5223; (*d*) E. H. A. Beckers, S. C. J. Meskers, A. P. H. J. Schenning, Z. Chen, F. Würthner, P. Marsal, D. Beljonne, J. Cornil and R. J. Janssen, *J. Am. Chem. Soc.*, 2006, **128**, 649–657; (*e*) A. Herrman, T. Weil, V. Sinigersky, U. M. Wiesler, T. Wosch, J. Hofkens, F. C. De Schryver and K. Mullen, *Chem.–Eur. J.*, 2001, **7**, 4844–4853; (*f*) R. F. Kelley, M. J. Tauber and M. R. Wasielewski, *J. Am. Chem. Soc.*, 2006, **128**, 4779–4791; (*g*) G. P. Wiederrecht, M. P. Niemczyk, W. A. Svec and M. R. Wasielewski, *J. Am. Chem. Soc.*, 1996, **118**, 81–88; (*h*) S. I. Yang, S. Prathapan, M. A. Miller, J. Seth, D. F. Bocian, J. S. Lindsey and D. Holten, *J. Phys. Chem. B*, 2001, **105**, 8249–8258; (*i*) M. E. El-Khouly, J. H. Kim, K.-Y. Kay, C. S. Choi, O. Ito and S. Fukuzumi, *Chem.–Eur. J.*, 2009, **15**, 5301–5310; (*j*) S. Xiao, M. E. El-Khouly, Y. Li, Z. Gan, H. Liu, L. Jiang, Y. Araki, O. Ito and D. Zhu, *J. Phys. Chem. B*, 2005, **109**, 3658–3667; (*k*) O. Johansson, M. Borgström, R. Lomoth, M. Palmblad, J. Bergquist, L. Hammarström, L. Sun and B. Åkermark, *Inorg. Chem.*, 2003, **42**, 2908–2918; (*l*) K. Okamoto, Y. Mori, H. Yamada, H. Himahori and S. Fukuzumi, *Chem.–Eur. J.*, 2004, **10**, 474–483; (*m*) R. F. Kelley, W. S. Shin, B. Rybtchinski, L. E. Sinks and M. R. Wasielewski, *J. Am. Chem. Soc.*, 2007, **129**, 3173–3181; (*n*) E. Iengo, G. D. Pantos, J. K. M. Sanders, M. Orlandi, C. Chiorboli, S. Fracasso and F. Scandola, *Chem. Sci.*, 2011, **2**, 676–685; (*o*) J. Baffreau, S. Leroy-Lhez, N. Vân Anh, R. M. Williams and P. Hudhomme, *Chem.–Eur. J.*, 2008, **14**, 4974–4992; (*p*) M. Wolffs, N. Delsuc, D. Veldman, N. Vân Anh, R. M. Williams, S. C. J. Meskers, R. A. J. Janssen, I. Huc and A. P. H. J. Schenning, *J. Am. Chem. Soc.*, 2009, **131**, 4019–4829; (*q*) A. Tolkki, E. Vuorima, V. Chukharev, H. Lemmetyinen, P. Ihalainen, J. Peltonen, V. Dehm and F. Würthner, *Langmuir*, 2010, **26**, 6630–6637; (*r*) Y. Wu, Y. Zhen, Z. Wang and H. Fu, *J. Phys. Chem. A*, 2013, **117**, 1712–1720.

5 (*a*) L. Flamigni, M. R. Johnston and L. Giribabu, *Chem.–Eur. J.*, 2002, **8**, 3938–3947; (*b*) L. Flamigni, E. Baranoff, J.-P. Collin and J.-P. Sauvage, *Chem.–Eur. J.*, 2006, **12**, 6592–6606; (*c*) L. Flamigni, B. Ventura, C.-C. You, C. Hippius and F. Würthner, *J. Phys. Chem. C*, 2007, **111**,

 This journal is © The Royal Society of Chemistry and Owner Societies 2013

622–630; (*d*) A. I. Oliva, B. Ventura, F. Würthner, A. Camara-Campos, C. A. Hunter, P. Ballester and L. Flamigni, *Dalton Trans.*, 2009, 4023–4037; (*e*) L. Flamigni, D. Wyrostek, R. Voloshchuk and D. T. Gryko, *Phys. Chem. Chem. Phys.*, 2010, **12**, 474–483.

6 (*a*) F. Würthner, S. Ahmed, C. Thalacker and T. Debaerdemaeker, *Chem.–Eur. J.*, 2002, **8**, 4742–4750; (*b*) N. Sakai, J. Mareda, E. Vauthey and S. Matile, *Chem. Commun.*, 2010, **46**, 4225–4237; (*c*) F. Würthner, *Chem. Commun.*, 2004, 1564–1579; (*d*) T. Weil, T. Vosch, J. Hofkens, K. Peneva and K. Müllen, *Angew. Chem., Int. Ed.*, 2010, **49**, 9068–9093; (*e*) X. Zhan, A. Facchetti, S. Barlow, T. J. Marks, M. A. Ratner, M. R. Wasielewski and S. R. Marder, *Adv. Mater.*, 2011, **23**, 268–284; (*f*) H. Langhals, *Helv. Chim. Acta*, 2005, **88**, 1309–1343; (*g*) J. Q. Qu, N. G. Pschirer, D. J. Liu, A. F. C. De Schryver and K. Mullen, *Chem.–Eur. J.*, 2004, **10**, 528–537; (*h*) H. Langhals, *Heterocycles*, 1995, **40**, 477–500; (*i*) Z. Chen, A. Lohr, C. R. Saha-Möller and F. Würthner, *Chem. Soc. Rev.*, 2009, **38**, 564–584; (*j*) C. Li and H. Wonneberger, *Adv. Mater.*, 2012, **24**, 613–636; (*k*) F. N. Castellano, *Dalton Trans.*, 2012, **41**, 8493–8501; (*l*) U. Selig, P. Nuernberger, V. Dehm, V. Settels, M. Gsänger, B. Engels, F. Würthner and T. Brixne, *ChemPhysChem*, 2013, **14**, 1413–1422.

7 H. Langhals, B. Böck, T. Schmid and A. Marchuk, *Chem.–Eur. J.*, 2012, **18**, 13188–13194.

8 L. Flamigni, A. Zanelli, H. Langhals and B. Böck, *J. Phys. Chem. A*, 2012, **116**, 1503–1509.

9 B. Ventura, H. Langhals, B. Böck and L. Flamigni, *Chem. Commun.*, 2012, **48**, 4226–4228.

10 L. Flamigni, A. I. Ciuciu, H. Langhals, B. Böck and D. T. Gryko, *Chem.–Asian J.*, 2012, **7**, 582–592.

11 R. A. Marcus, *Angew. Chem., Int. Ed. Engl.*, 1993, **32**, 1111–1121 and references therein.

12 (*a*) C. Flors, I. Oesterling, T. Schnitzler, E. Fron, G. Schweitzer, M. Sliwa, A. Herrmann, M. van der Auweraer, F. C. de Schryver, K. Müllen and J. Hofkens, *J. Phys. Chem. C*, 2007, **111**, 4861–4870; (*b*) A. Prodi, C. Chiorboli, F. Scandola, E. Iengo, E. Alessio, R. Dobrawa and F. Würthner, *J. Am. Chem. Soc.*, 2005, **127**, 1454–1462; (*c*) M. Tasior, D. T. Gryko, J. Shen, K. M. Kadish, T. Becherer, H. Langhals, B. Ventura and L. Flamigni, *J. Phys. Chem. C*, 2008, **112**, 19699–19709; (*d*) L. Flamigni, B. Ventura, A. Barbieri, H. Langhals, F. Wetzel, K. Fuchs and A. Walter, *Chem.–Eur. J.*, 2010, **16**, 13406–13413; (*e*) R. Voloshchuk, D. T. Gryko, M. Chotkowski, A. I. Ciuciu and L. Flamigni, *Chem.–Eur. J.*, 2012, **18**, 14845–14859; (*f*) H. Langhals, A. Obermeier, Y. Floredo, A. Zanelli and L. Flamigni, *Chem.–Eur. J.*, 2009, **15**, 12733–12744; (*g*) L. Flamigni, B. Ventura, M. Tasior, T. Becherer, H. Langhals and D. T. Gryko, *Chem.–Eur. J.*, 2008, **14**, 169–183; (*h*) C. Hippius, I. H. M. van Stokkum, E. Zangrando, R. M. Williams, M. Wykes, D. Beljonne and F. Würthner, *J. Phys. Chem. C*, 2008, **112**, 14626–14638.

13 H. Langhals, A. J. Esterbauer, A. Walter, E. Riedle and I. Pugliesi, *J. Am. Chem. Soc.*, 2010, **132**, 16777–16782.

14 H. Langhals, S. Poxleitner, O. Krotz, T. Pust and A. Walter, *Eur. J. Org. Chem.*, 2008, 4559–4562.

15 A. Weller, *Z. Phys. Chem. NF*, 1982, **133**, 93–98.

16 L. Hammarström, F. Barigelletti, L. Flamigni, N. Armaroli, A. Sour, J.-P. Collin and J.-P. Sauvage, *J. Am. Chem. Soc.*, 1996, **118**, 11972–11973.

17 Th. Förster, *Discuss. Faraday Soc.*, 1959, **27**, 7–17.

18 D. L. Dexter, *J. Chem. Phys.*, 1953, **21**, 836–850.

19 W. Van Der Meer, G. Coker and S. Y. Simon Chen, in *Resonance Energy Transfer Theory and Data*, VCH, Cambridge, 1994, p. 55–83.

20 κ^2 can be written as $\kappa^2 = (\cos\theta_T - 3\cos\theta_D \cos\theta_A)^2$,[19] where θ_D and θ_A are the angles formed between the line connecting the donor and acceptor centers and the transition moments of the donor and acceptor, respectively. θ_T is the angle between the transition moments of the donor and the acceptor. The transition moment of PI0 is oriented along the long axis and we assume the orientation of PIa to make an angle of *ca.* 45° with the line connecting the centers of the two reactant. In this conditions a κ^2 of 2 can be calculated.

21 (*a*) S. K. Lee, Y. Zu, A. Herrmann, Y. Geerts, K. Müllen and A. J. Bard, *J. Am. Chem. Soc*, 1999, **121**, 3513–3520; (*b*) J. E. Bullock, M. T. Vagnini, J. Ramanan, D. T. Co, M. Wilson, J. W. Dicke, T. J. Marks and M. K. Wasieliewski, *J. Phys. Chem. B*, 2010, **114**, 1794–1802.

22 L. Flamigni, A. M. Talarico, S. Serroni, F. Puntoriero, M. J. Gunter, M. R. Johnston and T. P. Jeynes, *Chem.–Eur. J.*, 2003, **9**, 2649–2659.

23 Matlab 5.2, The MathWorks Inc., Natick, MA, USA, 1998.

Published on 07 October 2013.